Influence of magnetic-field inhomogeneity on nonlinear magneto-optical resonances

S. Pustelny
Centrum Badań Magnetooptycznych, M. Smoluchowski Institute of Physics, Jagiellonian University, Reymonta 4, 30-059 Kraków, Poland

D. F. Jackson Kimball
Department of Physics, California State University-East Bay, 25800 Carlos Bee Boulevard, Hayward, California 94542, USA

S. M. Rochester
Department of Physics, University of California at Berkeley, Berkeley, California 94720-7300, USA

V. V. Yashchuk
Advanced Light Source Division, Lawrence Berkeley National Laboratory, Berkeley, California 94720, USA

D. Budker
Department of Physics, University of California at Berkeley, Berkeley, California 94720-7300, USA
and Nuclear Science Division, Lawrence Berkeley National Laboratory, Berkeley, California 94720, USA
(Received 9 August 2006; published 12 December 2006)

In this work, a sensitivity of the rate of relaxation of ground-state atomic coherences to magnetic-field inhomogeneities is studied. Such coherences give rise to many interesting phenomena in light-atom interactions, and their lifetimes are a limiting factor for achieving better sensitivity, resolution, or contrast in many applications. For atoms contained in a vapor cell, some of the coherence-relaxation mechanisms are related to magnetic-field inhomogeneities. We present a simple model describing relaxation due to such inhomogeneities in a buffer-gas-free antirelaxation-coated cell. A relation is given between relaxation rate and magnetic-field inhomogeneities including the dependence on cell size and atomic species. Experimental results, which confirm predictions of the model, are presented. Different regimes, in which the relaxation rate is equally sensitive to the gradients in any direction and in which it is insensitive to gradients transverse to the bias magnetic field, are predicted and demonstrated experimentally.

DOI: 10.1103/PhysRevA.74.063406 PACS number(s): 32.60.+i, 32.80.Bx, 42.65.−k

I. INTRODUCTION

In recent years, there has been considerable interest in many physical phenomena associated with the existence of coherence between atomic states. Such coherences, induced and detected by light, form the basis of certain nonlinear optical effects and are essential in such applications as magnetometry [1–6], electromagnetically induced transparency [7,8], and quantum gates [9]. They are also extensively employed in tests of fundamental symmetries (see, for example, the reviews [10,11]) and in frequency standards [12].

The lifetime of atomic coherences involving excited atomic states is generally limited to twice the time required for spontaneous emission of a photon and transition to a lower state. On the other hand, for coherences between atomic ground states, the effective coherence lifetime τ is either determined by the interaction time between the light and atoms, or by the time between coherence-destroying collisions. In many applications, the longer the lifetime of the coherences, the better resolution, contrast, or sensitivity that can be achieved.

In a typical experiment, involving a single light beam and a glass cell containing only alkali-metal vapor at low pressure, the effective coherence lifetime is given by the transit time of the atoms through the light beam. In order to suppress coherences-destroying collisions of atoms with cell walls and increase the lifetime τ, one of two methods is employed. The first method is to add to the cell a buffer (usually noble) gas at relatively high pressure. Since in the first approximation the collisions with the buffer gas are elastic, τ is then given by the time for the alkali-metal atoms to diffuse from the light beam. The second method is to apply an antirelaxation coating to the inner walls of the cell, preventing spin-depolarizing collisions of the atoms with the walls. This allows atoms to leave the light beam and later return to it with the coherences intact. Using these methods, the coherence lifetimes have been prolonged to hundreds of milliseconds (see, for example, Refs. [13,14] and references therein). As wall relaxation is decreased, however, other sources of relaxation become important, such as spin-exchange self-collisions and magnetic-field gradients, of which the latter is discussed here.

The sensitivity of the rate of relaxation γ of the ground-state coherences ($\gamma=1/\tau$) to magnetic-field inhomogeneities was previously studied under different experimental conditions [15–18]. In a series of papers [15], the sensitivity of the relaxation rate to the magnetic-field gradients was analyzed in antirelaxation-coated cells. Theoretical predictions supported by numerical simulations were compared with data obtained in a high-resolution Zeeman spectroscopy experiment performed with relatively strong bias magnetic field $B=50$ G. In such a range of magnetic fields, the nonlinear Zeeman effect contributes significantly to relaxation and it cannot be neglected. In Refs. [16–18], the sensitivity of the relaxation rate γ to the magnetic-field gradients in a buffer-gas cell was studied both theoretically and experimentally.

In this work, the rate of relaxation due to magnetic-field inhomogeneity is studied in buffer-gas-free antirelaxation-coated cells at relatively low magnetic fields ($|B| < 160$ mG), where the influence of the nonlinear Zeeman effect on relaxation is negligible. A naive theoretical model of the sensitivity of the relaxation rate to the magnetic-field inhomogeneity is given. A relation between the sensitivity of the relaxation rate and cell size or atomic spice contained in the cell is derived. Experimentally, the problem is studied using nonlinear magneto-optical rotation with frequency-modulated light (FM NMOR) [6]. The sensitivity of the FM NMOR resonances to first-order magnetic-field gradients is analyzed and compared with the model predictions. The sensitivity to the magnetic-field gradients is studied for different bias magnetic fields. This enables the observation of two different regimes, one in which the rate of relaxation γ depends equally on the magnetic-field inhomogeneities in each direction, and another in which it is completely insensitive to the transverse inhomogeneities.

The paper is organized as follows. In Sec. II, the theoretical model of the sensitivity of the rate of relaxation to the magnetic-field inhomogeneities is given. The experimental apparatus and the measurement technique are described in Sec. III. In Sec. IV, the experimental results are presented and compared with the predictions of the model. Conclusions are summarized in Sec. V.

II. THEORETICAL MODEL

Consider atoms contained in a buffer-gas-free, antirelaxation-coated spherical cell of radius R. Since at room temperature at saturated alkali-metal-vapor densities an atom's mean free path is on the order of hundreds of meters, the atoms travel freely between collisions with the cell walls. To analyze the influence of magnetic-field inhomogeneities on the rate of relaxation of the ground-state coherences, we use a simple model for a first-order magnetic-field gradient, for example $\partial B_i/\partial x_i$ in which the gradient field in each half of the cell is replaced by a constant magnetic field ΔB_i in that half. In other words, the cell is considered to have the magnetic field $\Delta B_i=(3R/8)(\partial B_i/\partial x_i)$ for $x_i>0$ and the opposite field $-\Delta B_i$ for $x_i<0$. At this point, we assume that ΔB_i is the only magnetic field inside the cell. However, the effect of homogeneous bias magnetic field **B** is considered below.

Between wall collisions, the atomic spins precess due to the magnetic field and acquire an average phase

$$\phi_{\text{grad}} \approx \frac{g\mu_B \Delta B_i \tau_c}{\hbar}, \tag{1}$$

where g is the Landé factor, μ_B is the Bohr magneton, and $\tau_c \approx 4R/3v$ is the average time between two collisions, and v is the rms atomic thermal velocity. However, since acquiring the phase is a random process, the actual phases acquired by the atom vary between collisions.

Another source of random phase is inelastic wall collisions. A simple model of wall-collision relaxation is the following. During a collision with the wall, an atom is stuck to the surface for approximately 10^{-10} s [19] (note that the duration of an elastic collision is $\sim 10^{-12}$ s), and is then released in a random direction with a random velocity. During the time it spends on the surface, the atom feels an excess magnetic field B_{wall}. This field causes the atomic spin to rotate, producing an average phase shift ϕ_{wall}. Combining the phases due to the magnetic-field inhomogeneity and wall collisions for N successive bounces in quadrature, the total phase is

$$(\phi_{\text{total}})^2 = N[(\phi_{\text{grad}})^2 + (\phi_{\text{wall}})^2]. \tag{2}$$

A characteristic relaxation time corresponds to a decrease of initial spin polarization by a factor of e. One can show that this happens when $\phi_{\text{total}}=\sqrt{2}$, and thus the total number of wall collisions before dephasing N_γ is

$$N_\gamma = \frac{\sqrt{2}}{(\phi_{\text{grad}})^2 + (\phi_{\text{wall}})^2}. \tag{3}$$

The relaxation rate γ of the atoms can be written as

$$\gamma = \frac{1}{N_\gamma \tau_c}. \tag{4}$$

In the two limiting cases in which only one mechanism of relaxation is present, Eq. (4) takes the forms

$$\gamma_{\text{grad}} = \frac{1}{N_{\text{grad}} \tau_c}, \tag{5}$$

$$\gamma_{\text{wall}} = \frac{1}{N_{\text{wall}} \tau_c}, \tag{6}$$

where N_{grad} and N_{wall} are, respectively, the numbers of bounces before relaxation when only the gradient relaxation or the wall relaxation is present. It is noteworthy that including other relaxation mechanisms such as spin-exchange collisions does not change the present treatment.

Combining Eqs. (1) and (3)–(6), we find

$$\gamma \approx \frac{4\mu_B^2 g^2 R \Delta B_i^2}{3\sqrt{2}\hbar^2 v} + \gamma_{\text{wall}} = \xi g^2 R^3 \left(\frac{\partial B_i}{\partial x_i}\right)^2 + \gamma_{\text{wall}}, \tag{7}$$

where $\xi = 3\mu_B^2/(16\sqrt{2}\hbar^2 v)$. One sees that the rate of relaxation due to magnetic-field gradients depends quadratically on the inhomogeneity of the magnetic field $(\partial B_i/\partial x_i)^2$, scales as R^3, and depends on the atomic species through the g^2 dependence.

Now, we consider the effect of the homogeneous bias magnetic field **B**, leading to a Larmor precession frequency $\Omega_L = g\mu_B B^\hbar$. In this situation, we consider two regimes: (i) $\Omega_L R/v \ll 1$, in which atomic spins rotate by only a small angle between collisions with the cell walls, and (ii) $\Omega_L R/v \gg 1$, in which the spins rotate by a large angle between successive wall bounces. In the first regime, since small rotations commute, i.e., the result of the composite rotation does not depend on the order of rotations, the spins' precession around orthogonal components of the magnetic field can be, to a good approximation, considered as independent. Thus, comparable sensitivity to longitudinal and transverse magnetic-field gradients can be expected. In the second regime, the Larmor precession is rapid and the strong

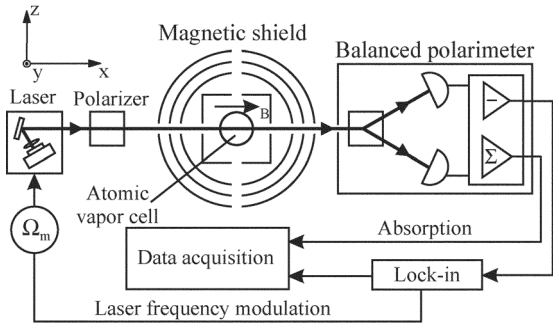

FIG. 1. Experimental setup. The magnetic-field coils enabling generation of bias magnetic field along x and compensation of the residual fields in other directions, as well as gradient coils, are not shown.

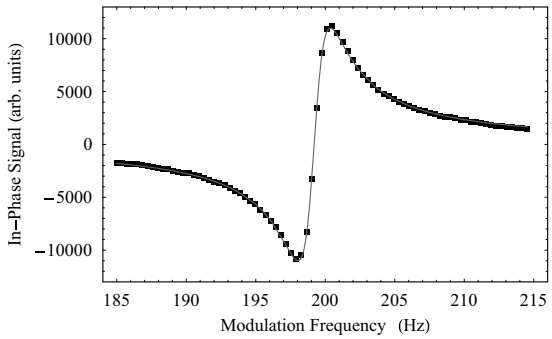

FIG. 2. A typical in-phase FM NMOR signal recorded in Rb10 cell. Square points represent experimental data. The solid line is a dispersive Lorentzian fit. The data were recorded in a single-beam experiment with the light power 4 μW and magnetic field corresponding to $\Omega_L \approx 2\pi \times 100$ Hz.

bias magnetic field breaks the symmetry of the system. Since fields transverse to the strong bias fields are only second-order corrections to the total magnetic field, the sensitivities of atomic-polarization relaxation rates to longitudinal and transverse magnetic-field gradients are different.

In the limit of high bias field, one would expect the relaxation rate to become completely insensitive to transverse gradients. However, according to Maxwell's equations, generation of a magnetic-field gradient in one direction requires gradients in other directions ($\nabla \cdot \mathbf{B} = 0$). Thus, in conditions of our experiment, when a gradient transverse to the light propagation direction is applied (say $\partial B_y / \partial y$), a gradient $\partial B_x / \partial x$ given by

$$\frac{\partial B_x}{\partial x} = -\frac{1}{2}\frac{\partial B_y}{\partial y} \tag{8}$$

also appears along the longitudinal direction x. Since the relaxation is quadratic in the magnetic-field gradient, it is expected that the relaxation rate should be four times as sensitive to gradients nominally along the longitudinal direction as they are to those nominally in a transverse direction.

III. EXPERIMENTAL SETUP

Relaxation rates may be studied by observing the widths of resonances in optical rotation using the FM NMOR technique [6]. The layout of the experimental setup is shown in Fig. 1. Rubidium atoms are contained in antirelaxation-coated buffer-gas-free spherical vapor cells of different diameters and containing different isotopic compositions of rubidium (Table I) [24].

TABLE I. Antirelaxation-coated, buffer-gas-free vapor cells used in the present work.

Cell designation	Outer diameter (cm)	Isotope
Ale10	10.0(1)	^{85}Rb
Rb10	10.2(1)	^{87}Rb
Gibb	10.3(3)	Natural Rb
H2	3.4(1)	^{87}Rb

A cell is placed inside a four-layer magnetic shield providing passive attenuation of the dc magnetic fields to the level of one part per 10^6 [20]. A set of three mutually orthogonal magnetic-field coils is mounted inside the innermost shielding layer. These coils are used for compensation of the residual magnetic field inside the shield, as well as for generating a bias magnetic field along the x axis. Data were taken for the bias magnetic field ranging from 0.2 to 155 mG. An additional set of three calibrated coils is used for compensation and generation of first-order magnetic-field gradients inside the shield.

The rubidium atoms interact with y-polarized light produced by an external-cavity diode laser operating at the rubidium $D1$ line (795 nm). The ~ 3 μW light beam is 2 mm in diameter and propagates along x. The laser light is frequency modulated at a rate $\Omega_m \approx 2\Omega_L$ with a modulation depth of 300 MHz (peak to peak). The central frequency of the laser is tuned to the low-frequency wing of the $F=2 \rightarrow F'=1$ transition for ^{87}Rb measurements and to the center of the $F=3 \rightarrow F'$ transition group for ^{85}Rb measurements, in order to produce the maximum FM NMOR signal in each case. The central frequency of the laser is stabilized with a dichroic atomic vapor lock [21,22] modified for operation with frequency-modulated light. The rotation of the polarization plane of the light transmitted through the vapor cell is analyzed with a balanced polarimeter (a crystalline polarizer rotated by 45° in the yz plane and two photodiode detectors). A photodiode difference signal is detected with a lock-in amplifier at the first harmonic of Ω_m. In-phase and quadrature components of the detected signal are stored with a computer.

Some of the results presented in this paper were recorded with an experimental arrangement slightly different from Fig. 1, essentially the same as the one described in Ref. [23]. Instead of one light beam, an additional unmodulated (probe) laser is used. The probe laser operating at the rubidium $D2$ line (780 nm) is tuned to the center of the $F=2 \rightarrow F'$ transition group of ^{87}Rb. It is polarized in the y direction, that is, in the same direction as the pump beam. The probe laser light propagates along x, while the frequency-modulated (pump) laser beam propagates along z. The polarization-plane rotation of the probe laser beam was measured with the polarim-

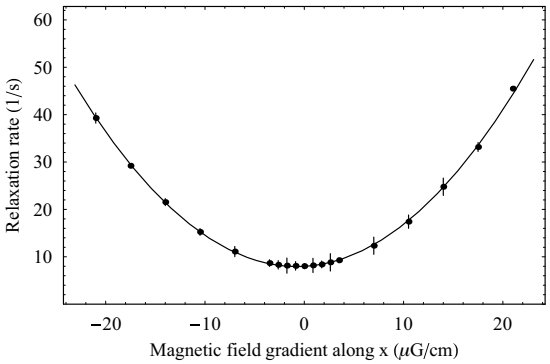

FIG. 3. Relaxation rate of the ground-state coherences, extracted from the width of the FM NMOR resonance, vs the first-order magnetic-field gradient applied using x-oriented coils. Note that the application of such a gradient is accompanied by the appearance of gradients in y and z directions (see text). The experimental results are fit with a quadratic dependence [Eq. (9)]. The signals were recorded in a single-beam arrangement in the Rb10 cell with bias magnetic field $B \approx 250$ μG and light power 4 μW.

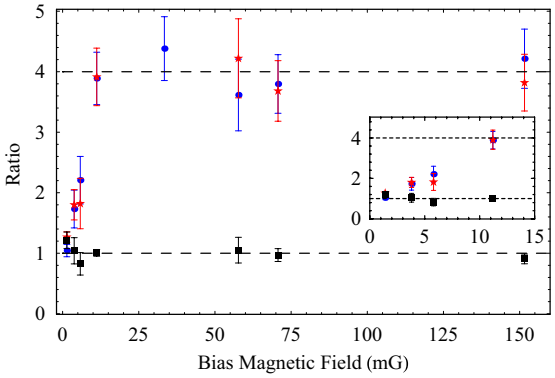

FIG. 4. (Color online) Ratio between sensitivity to the magnetic-field gradients generated with x, y, and z coils. Circles correspond to the ratio between sensitivities applied with x and y coils (a_x/a_y), stars with x and z coils (a_x/a_z), and squares with y and z coils (a_y/a_z). The data were recorded in a two-beam arrangement in the H2 cell. The pump- and probe-beam powers were 15 and 5 μW, respectively.

eter at the first harmonic of the pump-laser modulation frequency. Despite the changes in the experimental arrangement, the experimental results obtained in the one- and two-beam experiments are consistent.

IV. RESULTS AND ANALYSIS

A typical in-phase FM NMOR signal recorded as a function of a modulation frequency is shown in Fig. 2. Experimental data were fit with a dispersive Lorenzian. The width of the FM NMOR signal $\Delta\nu$, which corresponds to the relaxation rate of the ground-state coherences γ by the relation $\gamma = 2\pi \times \Delta\nu$, is half of the distance between two peaks in the signal.

In Fig. 3, the dependence of the rate of relaxation of the ground-state coherences γ is presented as a function of the magnetic-field gradients applied with x coils. In order to verify the predictions of the model, the experimental data were fit with the quadratic dependence,

$$\gamma = a_i \left(\frac{\partial B_i}{\partial x_i} \right)^2 + \gamma_0, \tag{9}$$

where a_i is the coefficient describing the sensitivity to the magnetic-field gradient applied using x_i-oriented coils and γ_0 is the relaxation rate in the absence of the gradients. As seen in Fig. 3, the experimental data are in good agreement with the theoretically predicted quadratic dependence of the relaxation rate as a function of the magnetic-field gradient. The agreement was also observed for two transverse directions y and z.

The sensitivities to the magnetic-field gradients were also studied as a function of the strength of the bias magnetic field. The ratios between sensitivities to gradients applied with x, y, and z coils are shown in Fig. 4. The sensitivity to the gradients applied with either of the transverse coils is the same ($a_y/a_z \approx 1$) over the whole range of bias magnetic fields, as expected by symmetry. However, as predicted in Sec. II, the ratio between the sensitivity to magnetic-field gradients applied with the longitudinal and transverse coils changes with the strength of the bias magnetic field. In the zero-field limit of the bias field, the sensitivity to the magnetic-field gradients applied with the longitudinal and either of the transverse coils is the same ($a_x/a_y \to 1$ and $a_x/a_z \to 1$). For stronger bias fields, the ratio between the sensitivity to the first-order magnetic-field gradients applied with the longitudinal and transverse coils increases until it levels off at $a_x/a_y \approx a_x/a_z \approx 4$ for $B > 15$ mG. These results are in agreement with the theory, which predicts $a_{\mathrm{long}}/a_{\mathrm{trans}} = 1$ for $\Omega_L R/v \ll 1$ and $a_{\mathrm{long}}/a_{\mathrm{trans}} = 4$ for $\Omega_L R/v \gg 1$. For the experimental conditions of Fig. 4, 15 mG corresponds to $\Omega_L R/v \approx 3$. Thus the experimental results confirm that for high bias fields, the rate of relaxation γ

TABLE II. Sensitivity of the relaxation rate to the magnetic-field gradients applied in a given direction. The bias magnetic field was $B \approx 250$ μG, except for Ale10, for which it was $B \approx 300$ μG. In the Gibb cell, the sensitivity to the magnetic-field gradients was measured for ^{87}Rb.

Cell	a_x (cm^2/s μG^2)	a_y (cm^2/s μG^2)	a_z (cm^2/s μG^2)
Rb10	83.6(7)	50.9(7)	47.7(7)
Gibb	89.2(13)	59.7(25)	52.8(13)
Ale10	32.0(7)	18.8(13)	18.2(7)
H2	2.2(4)	1.4(2)	1.6(2)

TABLE III. Ratio between the sensitivities to the magnetic-field gradients applied with coils oriented in a given direction for cells of different radii (upper subtable) and cells containing different isotopes of rubidium (lower subtable). The uncertainties in the ratio between sensitivity to the gradients in cells of different sizes represent deviations from a perfect spherical shape and uncertainty in the estimation of cell thickness. To calculate the ratios for different isotopes, the slight differences in the cell internal sizes were taken into account.

Cells	x axis	y axis	z axis	Theory
		Different radii		
Rb10/H2	40(8)	43(8)	33(4)	35(8)
Gibb/H2	38(8)	36(6)	30(5)	36(10)
Rb10/Gibb	0.94(3)	0.85(5)	0.90(4)	0.94(12)
		Different isotopes		
Ale10/Gibb	0.39(2)	0.34(4)	0.38(3)	0.44
Ale10/Rb10	0.41(2)	0.39(4)	0.41(3)	

is insensitive to the transverse part of the magnetic-field inhomogeneities.

Table II gives the sensitivity of the rate of relaxation of the ground-state coherences to magnetic-field gradients applied with each of the three gradient coils for the four cells studied here. The sensitivity to the magnetic-field gradients varies with the orientation of the coils used for the generation of the gradients, cell size, and rubidium isotope.

As seen in Table II, the sensitivity to the gradients in larger cells is stronger than in the smaller cell. According to Eq. (7), the sensitivity to the magnetic-field gradients scales as R^3. In order to check this, Table III gives the experimentally measured ratios for cells of different sizes along with the theoretical predictions. To calculate the theoretical ratio between sensitivity due to different sizes of the cells, their inner radii were used. They were estimated by subtraction of a wall thickness, which was assumed to be $\sim$0.2 cm, from the cells' outer radii.

The experimental data are consistent with the predictions of the model.

According to the model, the FM NMOR width scales with the Landé factor as g^2 [Eq. (7)]. For the two isotopes of rubidium, ^{85}Rb and ^{87}Rb, for which the Landé factors are 1/3 and 1/2, respectively, the expected ratio is 4/9. Rough agreement is seen between the experimental results and predictions for the ratios of sensitivities for cells containing different isotopes (Table III). The results in Table III are scaled to take into account the different cell sizes. For the results relating the Ale10 and Gibb cells, we associate a difference from the theoretical value with the slightly nonspherical shape of the Gibb cell (in addition to the overall nonsphericity, it does not have a typical stem but it has a number of tubulations). Another source of deviation is the different bias field used for the measurements with the Ale10 cell, as noted in the caption to Table II. As discussed above, this difference affects the sensitivities to the transverse magnetic-field gradients.

V. CONCLUSION

We have presented a simple model describing a relation between the relaxation rate of the ground-state coherences γ of atoms contained in buffer-gas-free antirelaxation-coated cell and magnetic-field inhomogeneities. The results of the experiments using nonlinear magneto-optical rotation with frequency-modulated light have confirmed the model across the board. We showed that the rate of relaxation γ of the ground-state Zeeman coherences is proportional to the square of the magnetic-field inhomogeneity (first-order magnetic-field gradients), and that it scales as the cube of the cell size and as the square of the Landé factor. Additionally, we provide experimental evidence that the sensitivity to the longitudinal part of the magnetic-field inhomogeneity is independent of bias magnetic field, but the sensitivity to the transverse part of the inhomogeneity changes with bias field. At small bias fields, the sensitivity to transverse inhomogeneities is similar to the sensitivity in the longitudinal direction, but at larger fields (where the Zeeman frequency exceeds the wall-collision rate), it vanishes.

ACKNOWLEDGMENTS

The authors would like to acknowledge H. Robinson for providing one of the cells, and E. B. Alexandrov, W. Gawlik, J. Higbie, M. Ledbetter, M. V. Romalis, and I. Savukov for helpful discussions. This work is supported by DOD MURI Grant No. N-00014-05-1-0406, KBN Grant No. 1 P03B 102 30, and a NSF U.S.-Poland collaboration grant. One of the authors (S.P.) is supported by the project cofinanced from the European Social Fund.

[1] E. B. Alexandrov, M. V. Balabas, A. K. Vershovski, and A. S. Pazgalev, Tech. Phys. **49**, 779 (2004).
[2] H. Gilles, J. Hamel, and B. Cheron, Rev. Sci. Instrum. **72**, 2253 (2001).
[3] A. Weis and R. Wynands, Opt. Lasers Eng. **43**, 387 (2005).
[4] D. Budker, V. Yashchuk, and M. Zolotorev, Phys. Rev. Lett. **81**, 5788 (1998).
[5] D. Budker, D. F. Kimball, S. M. Rochester, V. V. Yashchuk, and M. Zolotorev, Phys. Rev. A **62**, 043403 (2000).
[6] D. Budker, D. F. Kimball, V. V. Yashchuk, and M. Zolotorev, Phys. Rev. A **65**, 055403 (2002).
[7] E. Arimondo, Prog. Opt. **25**, 257 (1996).
[8] S. E. Harris, Phys. Today **50**, 36 (1997).
[9] Q. A. Turchette, C. J. Hood, W. Lange, H. Mabuchi, and H. J. Kimble, Phys. Rev. Lett. **75**, 4710 (1995).
[10] E. B. Alexandrov, M. Auzinsh, D. Budker, D. F. Kimball, S. M. Rochester, and V. V. Yashchuk, J. Opt. Soc. Am. B **22**, 7 (2005).
[11] D. Budker, W. Gawlik, K. F. Kimball, S. M. Rochester, V. V. Yashchuk, and A. Weis, Rev. Mod. Phys. **74**, 1153 (2002).
[12] J. Vanier, Appl. Phys. B **81**, 421 (2005).
[13] D. Budker, L. Hollberg, D. F. Kimball, J. Kitching, S. Pustelny, and V. V. Yashchuk, Phys. Rev. A **71**, 012903 (2005).
[14] M. Erhard and H. Helm, Phys. Rev. A **63**, 043813 (2001).
[15] S. F. Watanabe and H. G. Robinson, J. Phys. B **10**, 931 (1977); **10**, 941 (1977); **10**, 959 (1977); **10**, 1198 (1977).
[16] G. D. Cates, S. R. Schaefer, and W. Happer, Phys. Rev. A **37**, 2877 (1988).
[17] D. D. McGregor, Phys. Rev. A **41**, 2631 (1990).
[18] C. L. Bohler and D. D. McGregor, Phys. Rev. A **49**, 2755 (1994).
[19] M. A. Bouchiat and J. Brossel, Phys. Rev. **147**, 41 (1966).
[20] D. Budker, V. V. Yashchuk, and M. Zolotorev, in *Trapped Charged Particles and Fundamental Physics*, edited by D. H. E. Dublin and D. Schneider (American Institute of Physics, New York, 1999), pp. 177–182.
[21] K. L. Corwin, Z.-T. Lu, C. F. Hand, R. J. Epstain, and C. Wieman, Appl. Opt. **37**, 3295 (1998).
[22] V. V. Yashchuk, D. Budker, and J. R. Davis, Rev. Sci. Instrum. **71**, 341 (2000).
[23] S. Pustelny, D. F. Jackson Kimball, S. M. Rochester, V. V. Yashchuk, W. Gawlik, and D. Budker, Phys. Rev. A **73**, 023817 (2006).
[24] The cells used in this work were previously intensively studied in different experiments. A detailed analysis of hyperfine and Zeeman relaxations in these cells is presented in Ref. [13].